Chapter 29
Imaging After Neoadjuvant Therapy

Eva-Maria Gassner, Paulina Poskaite, and Werner Jaschke

Take Home Messages

- After neoadjuvant therapy, most patients show stable disease at imaging and about 20% have partial response. Progression of disease is reported in about 16%.
- Cross-sectional imaging overestimates the amount of residual viable tumour around vessels and thus cannot reliably predict resectability
- Functional imaging may depict tumour activity under therapy, but currently lacks the spatial resolution to detect microscopic disease at the crucial interface of mass and vessel wall

Pearls and Pitfalls

- After neoadjuvant therapy, a persistent tissue cuff around crucial vessels is not correlated to histopathologic margins
- There is no consensus on absolute sizes, size dynamics or grey level intensities predicting margin-free resection; most research focuses on tumours of less than 3 cm.
- Imaging correlates of tumour biology under therapy are increasingly investigated

E.-M. Gassner (✉) · P. Poskaite · W. Jaschke
Department of Radiology, Medical University Innsbruck, Innsbruck, Austria
e-mail: eva.gassner@tirol-kliniken.at

K. Søreide, S. Stättner (eds.), *Textbook of Pancreatic Cancer*,
https://doi.org/10.1007/978-3-030-53786-9_29

Future Perspectives

- Detection of subtle changes after therapy needs enhanced tissue differentiation on CT and better special resolution in functional imaging (diffusion-weighted MRI and PET-CT)
- Several methods of diffusion-weighted imaging are tested to increase specificity for residual tumour versus inflammation and oedema, the most widely investigated being intravoxel incoherent motion (IVIM) diffusion-weighted imaging (DWI)
- Quantifying tumour heterogeneity with texture analysis software tools is another thriving approach to translate tumour behaviour into imaging ('radiomics' science).

29.1 Introduction

Pancreatic Ductal Adenocarcinoma (PDAC) is categorized into three surgical stages at the time of diagnosis if no distant metastasis is present: resectable, borderline resectable, and locally advanced [1], and the benefit of neoadjuvant therapy on pancreatic adenocarcinoma is currently subject of intensive clinical research [2, 3]. Since the recognition of borderline resectable disease in 2008 [4], neoadjuvant concepts have been implemented in order to achieve downstaging from either borderline resectable or locally advanced/non-resectable PDAC to a more favourable surgical stage, while in a more recent development, neoadjuvant therapy in the setting of resectable PDAC has equally gained momentum [5–7]. Gemcitabine-based regimens combined with nab-paclitaxel [8], and the advent of FOLFIRINOX-based schemes in 2011 [9], both with or without additional chemoradiation, hold promise for downstaging PDAC and more importantly, enhance the rate of margin-free (R0) resection [10–12].

Unfortunately, response evaluation on imaging and prediction of resectability has proven challenging due to inhomogeneous tumour replacement, mainly by fibrosis [13]. Although CA 19-9 levels and clinical performance status are incorporated into reassessment [1], multiphase contrast-enhanced multidetector CT (MDCT) with three-dimensional reconstructions remains the mainstay for further patient selection for surgery [14]. Meanwhile, advances in magnetic resonance imaging (MRI), notably faster acquisition techniques and enhanced image quality have brought MRI close to the spatial resolution of MDCT, while offering superior contrast resolution and the opportunities of functional imaging in terms of diffusion-weighted imaging (DWI) [15].

29.2 Impact of Histopathologic Response Patterns on Imaging

It was early recognized that NAT-induced tumour cell injury in PDAC is mainly reflected by isovolumetric tissue replacement with fibrous stroma, inflammation and extracellular matrix, rather than volume loss [13, 16]. In 1992, Evans at al.

reported the histologic changes in 17 resected specimens after NAT and established a pathologic response grading system for PDAC [17] by describing the percentage of viable tumour cells within the specimen. However, Evan's proposal is derived from response assessment in other organ systems, causing some criticism over hypothesized analogies to adenocarcinomas of the pancreas [18]. In their review, Kalimuthu et al. outlined histopathologic changes after NAT with emphasis on subtle residual tumour nests scattered throughout fibrosis [19].

New insights into the biology of PDAC reveal complex interactions of stroma, extracellular matrix, inflammation, and tumour cells [20]. This histopathologic heterogeneity of response, and non-discernible microstructure invasion is thought to cause failures in predicting viable tumour around crucial surgical structures [21–24]. Meta-analyses of histopathology after NAT of note, found lower rates of perineural invasion [11, 25] and a rate of complete pathologic response of 2–7% [26, 27].

29.3 Imaging Response Assessment with RECIST1.1 (Clinical Stage)

Owing to the specific tumour spread of PDAC, metric re-assessment using RECIST1.1 guideline is widely perceived as a suboptimal approach, although currently without alternative [28] for estimating response (Table 29.1).

In a meta-analysis, overall RECIST1.1 response rate after neoadjuvant therapy were available for 61 studies [29], and pooled pathologic tumour destruction grades for 36 studies. Overall, the majority of patients were stable or in partial response on cross-sectional imaging (Table 29.2), and, upon available pathologic grading, most of the resected specimens showed minor to moderate histologic response (<50% tumour destruction, Table 29.3).

However, radiologic and pathologic grading are not correlated on a per-patient basis [30]. In a work-up of 38 specimens after NAT, all pathologic tumour

Table 29.1 RECIST1.1 definitions of imaging response

Category	RECIST1.1 classification
Complete response (CR)	No visible tumor
Partial response (PR)	≥30% decrease
Stable disease (SD)	Neither PR nor PD
Progressive disease (PD)	≥20% increase from best time point

Table 29.2 RECIST1.1 response rates on imaging after neoadjuvant therapy in a meta-analysis by Dhir et al. [29]

RECIST1.1 response rates after neoadjuvant therapy			
CR	PR	SD	PD
<1%	20%	59%	16%

Percentages display overall response rates from 61 studies; included are patients with resectable, borderline resectable and locally advanced PDAC

Table 29.3 Pathologic response from resected specimen in the same meta-analysis [29]

Pathologic overall response in resected specimen after neoadjuvant therapy					
Tumor destruction rate	<10%	10–50%	50–90%	<90%	No viable tumor
Frequencies (percentages)	12%	37%	27%	13%	3%

Table 29.4 Pathology-imaging correlation: Distribution of RECIST1.1 imaging response and pathologic tumor destruction grades in resected specimen, as found in the publication by Xia et al. [30]

	RECIST 1.1 response (n = 38)			
Pathologic tumor destruction grade	CR n = 1	PR n = 10	SD n = 26	PD n = 1
<50%		5	19	1
50–90%	1	3	4	
>90%		1	1	
No viable tumor		1	2	

destruction grades from minimal to complete were found in both radiologic partial responders and in patients with stable disease. Pathologic response of <50% tumour destruction was dominant in the largest RECIST group of stable disease. Of note there were three pathologic complete responders out of 38 specimens, two with RECIST stable disease, and one with partial response (Table 29.4).

In the light of unsatisfactory results of tumour re-assessment with RECIST1.1, alternative determinants of response are being investigated. In such, therapy-induced sharp tumour demarcation at the interface to normal pancreas parenchyma was found useful to predict improved survival, although the magnitude of the effect varied across cohorts [31].

29.4 Imaging Assessment of Resectability

29.4.1 Clinical Impact of Patient Selection Based on Imaging

The advent of novel neoadjuvant concepts has triggered extensive research on radiologic tumour changes after therapy, with special attention to resectability. Meta-analyses suggest high R0 rates in patients with borderline resectable PDAC: when 65% of patients were selected for surgery after FOLFIRINOX, R0 margins resulted in overall 89% of them. On an intention-to-treat basis, this translates into free margins in 58% of treated patients [25]. Selection for surgery becomes even more important in locally advanced PDAC with neoadjuvant therapy [32]: when an overall 28% of patients were brought to surgery after FOLFIRINOX, free margins were seen in 74% of operated subjects, resulting in only 22% of R0 margins on an intention-to-treat basis [33, 34]. Generally, imaging workup after neoadjuvant therapy reveals an overestimation of residual tumour burden around vessels and the

probability of R0 resection is difficult to estimate. Diagnostic accuracy for predicting resectability after neoadjuvant therapy yielded an accuracy of 58% in a publication by a French group [35].

29.4.2 Neoadjuvant Therapy and R0 Resection in Study Settings

The effect of FOLFIRINOX on resectability criteria, compared to pathologic margins, was presented in two initial publications with similar results.

In a first retrospective single-centre study of 40 patients after FOLFIRINOX (14 borderline resectable, 26 locally advanced), a strong trend towards surgical downstaging could be observed. But while 19 patients still remained radiographically in the locally advanced group, R0 margins could be achieved in 35/40 patients (92%), thus including a large portion of patients with persistent non-resectable disease on CT [36].

A French multicentre study [37] noted downstaging of resectability in only 6/36 patients after FOLFIRINOX, while the majority of patients remained stable on imaging. However, R0 resections were seen in 31 patients (86%), among them six patients with persistent locally advanced disease on imaging.

Subsequent publications confirmed, that resectability guidelines are not applicable on treated PDAC, since unchanged perivascular cuffs after neoadjuvant therapy are not correlated to resection margins [38] (Fig. 29.1).

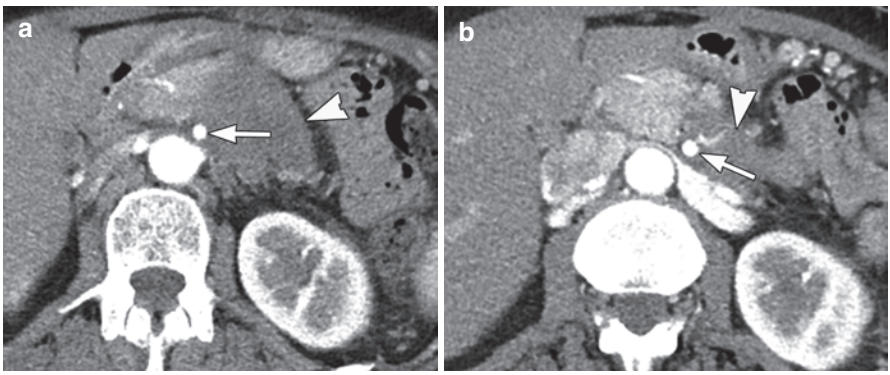

Fig. 29.1 Locally advanced PDAC under neo-adjuvant treatment. (**a**) Baseline image of a locally advanced PDAC in a 52-year-old female (arrowhead), with encasement of the superior mesenteric artery of >180° (arrow). (**b**) The same patient after neoadjuvant therapy with FOLFIRINOX. Considerable tumour shrinkage can be seen (arrowhead), however SMA encasement persists (arrow). The patient underwent total pancreatectomy with complete tumour dissection from the SMA and negative resection margins

29.4.3 Tested Predictors for Resectability and Survival After Neoadjuvant Therapy

Subsequently, several studies have focused on imaging predictors for margin-free surgery, with heterogeneous approaches and results.

29.4.3.1 Regression of Vessel Contact

A retrospective single-centre assessment of 47 patients found a regressive circumferential tumour contact with any of the crucial vessels (superior mesenteric vein, portal vein, superior mesenteric artery and celiac trunk) being predictive for R0 resections (PPV 91%). Specifically, a regression of circular SMA contact yielded an odds ratio of 3.82 (95% CI 1.27–11.5) for free margins [39]. Although a decrease in circumferential venous contact was also related to free margins, no correlation was observed between persistent narrowing of SMV/PV and R0 resection.

In a multicentre retrospective study on 36 patients [37], the circumferential decrease of perivascular cuffs did not reach significance levels when R0 and R1 resections were compared. However, patients with regressive encasement showed an advantage in disease-free survival, while the few patients with progressive encasement under therapy had significantly shorter disease-free survival.

29.4.3.2 Size and Resectability

Other studies published metric thresholds as predictors for negative margins. One of the largest single-institution retrospective studies with 141 patients found post-FOLFIRINOX differences in median size (2.3 cm vs. 3 cm) to be associated with attempted curative surgery (R0 in resected: 80%) [40]. Another publication revealed a 25 mm threshold after therapy, below which 78% of tumours had free margins [38]. Differences in size after treatment between R0 and R1 were observed in several publications (Table 29.5), but, using a linear correlation, post-treatment tumour

Table 29.5 Median/median tumor dimensions after neoadjuvant therapy and decrease in size, as reported in imaging studies after FOLFIRINOX

	Absolute dimension after neoadjuvant therapy (mm)		Size variability neoadjuvant therapy	
Study [Reference number]	R0	R1	R0	R1
Wagner et al. [37]	27	26	−65%	−56% (n.s.)
Marchegiani et al. [41]	21	26	−11 mm	−8 mm
Cassinotto et al. [39]	26	31	−7.6 mm	−7 mm
Michelakos et al. (median) [40]	23	30	−9 mm	0 mm

size was only weakly related to R0 margins [39]. There were considerable ranges of tumour sizes in tested populations both at baseline and post-treatment, consequently, dimensions associated with R0 or R1 resection are overlapping across studies. Noteworthy, the treatment-induced decrease in size was not significantly different between R0 and R1 patients (Table 29.5).

29.4.3.3 Tumour Enhancement

Increased enhancement under neoadjuvant therapy was observed in several studies and is attributed to fibrotic changes, similar to the delayed enhancement of myocardial infarcts in cardiac MRI or delayed enhancement of intrahepatic Cholangiocarcinoma, thought to represent fibrotic tumour components [41]. One retrospective single centre study found treatment-induced positive changes in enhancement in the venous phase being significantly higher in R0-resected tumours than in R1. However in other publications this treatment-effect was not significant [39] or even reversed with more pronounced density increases in R1 resected [37] (Table 29.6).

29.4.4 Study Characteristics of Imaging Predictor Assessment

In observational studies on PDAC morphology after therapy, patients proceeded to resection when they had stable disease or partial response on imaging. Imaging-progressive patients were excluded, and consequently, lack histological correlation. The decision to bring progressive patients to non-surgical palliation is based on high NPVs for assessing resectability in treatment naïve PDAC [41]. In an interesting aspect, one paper [40] reported two out of seven patients with post-treatment operability on CT, who eventually had non-resectable disease. This may suggest rare cases of underestimated local tumour extent.

Most publications are retrospective in design and, apart from the French [37] and Italian (three institutions) [38], all are single-centre.

Results of inter-observer concordance varied widely across publications, ranging from excellent in highly specialized centres [31] to only moderate κ-values of 0.57–0.58 [39]. In one publication, even the determination of a straightforward metric parameter, such as the longest axis, did not exceed a moderate κ-value of 0.54 among three radiologists with heterogeneous experience levels [38].

Table 29.6 Mean tumor enhancement (Hounsfield Units) before and after neoadjuvant therapy in R0 vs. R1 resected tumors

	Pre-treatment		Post-treatment	
Tumor enhancement during portal venous phase	R0	R1	R0	R1
Wagner et al. [37]	66	54	72	72
Marchegiani et al. [41]	62	65	78	68

Furthermore, resection margins of more than 1 mm were regularly used as a reference standard to evaluate the performance of cross-sectional imaging in treated PDAC. The histologic distribution of viable tumour within fibroinflammatory tissue has so far not been correlated to imaging on a lesion-by-lesion comparison.

29.5 Texture Analysis: Big Data Analysis in Imaging

29.5.1 Background

Radiomics, the mathematical exploitation of multiple background information contained in imaging data sets has gained momentum in recent years to quantitatively describe tumours before and after therapy. A most thriving application field of radiomics is CT/MR texture analysis to quantify visually non-perceptible heterogeneity [42, 43]. The method employs commercially available software to extract, on different complexity levels, quantitative descriptors such as distribution and statistical inter-relationship of grey levels from a Region of Interest (ROI). These input data are then processed to calculate parameters for quantifying tumour heterogeneity (Box 29.1). Validation of obtained output parameters (e.g. standard deviation of grey values, entropy, skewness, kurtosis, mean of the positive pixels) is performed by testing their association to histopathology and outcomes such as R0 resection or survival [44]. Descriptors may be derived from either CT, MRT or PET data sets.

Box 29.1 CT-Texture Analysis

CT Texture analysis is based on frequencies and inter-relationship of grey levels within an operator-determined Region of Interest (ROI, yellow circle). Input images first undergo pre-processing steps in order to selectively extract density features. Distribution and spatial variation of grey levels can be analysed using different models, with statistical-based models being most widely validated (Fig. 29.2a).

First order statistics describe grey-level frequencies, but do not refer to their spatial relationship. First order statistics are derived from intensity histograms representing grey level values on x-axis and their frequencies on y-axis. Histograms provide measures such as mean grey level (48 Hounsfield Units in this case), standard deviation and MPP (mean of positive pixels) to characterize a Region of Interest (Fig. 29.2b). Other first order statistics calculated from histograms are skewness (asymmetry of the histogram, left) and kurtosis (right, peakedness) compared to normal distribution. Energy (=uniformity, indicating how close the image is to a uniform Gaussian distribution) and first order entropy (irregularity of grey-level distribution in a histogram) are mathematically derived (Fig. 29.2c). Second-order statistics describe the spatial inter-relationship of intensities based on the probability of two or more pixel combinations in all directions (Fig. 29.2d).

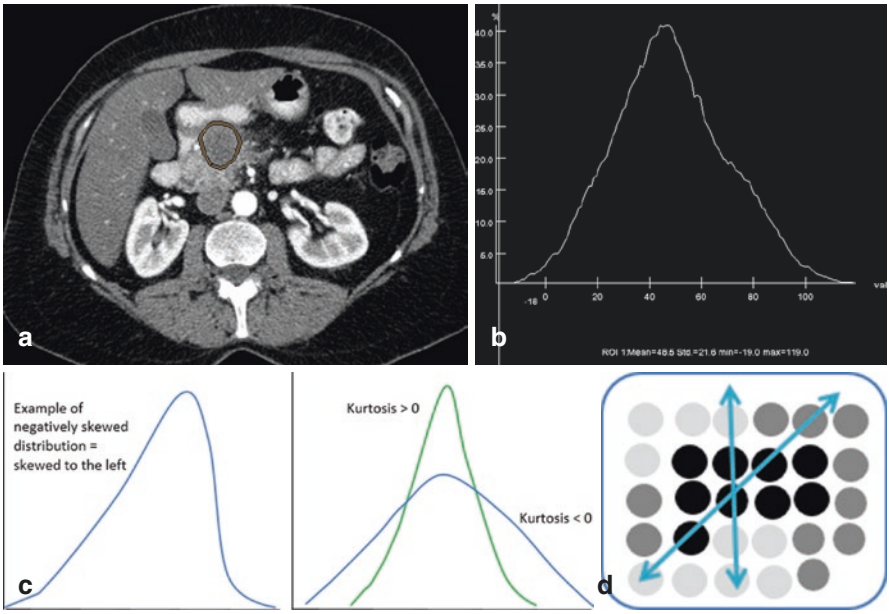

Fig. 29.2 (**a**–**d**) Principles of CT texture analysis

29.5.2 Application to Neoadjuvant Treatment of PDAC

Published data on the usefulness of CT Texture Analysis (CTTA) to estimate response in PDAC are preliminary. One group of investigators [45] tested a set of six CTTA parameters of 41 patients (mean grey-level intensity, entropy, mean of positive pixels, kurtosis, standard deviation, and skewness), together with tumour size and clinical variables in a multivariate regression model: two pre-treatment CTTA parameters, standard deviation and skewness were associated to survival. However, tumour size as a readily available parameter yielded higher significance levels than CTTA variables. In contrast to pre-treatment texture parameters, neither post-treatment values, nor their changes were associated to clinical outcomes.

Despite rapidly growing publication counts, radiomics need further standardization to provide inter-institutional reproducibility [44, 46]. Each step in the automated process is still dependent on variables, such as quality of input images, definition of parameters, robustness of extraction and statistical model building [47].

29.6 Functional Imaging: Diffusion-Weighted MRI for Monitoring Response

29.6.1 Current Application and Results

Diffusion-weighted MR imaging (DWI) offers functional tissue assessment by mapping the restriction of random (Brownian) molecule motion in water. Diffusion restriction is a marker for cellularity and pathologic characteristics of cellular barriers, both increased in tumours [48] (see also MR/MRCP for diagnosis and staging). Calculating apparent diffusion coefficients (ADC) in multiples of 10^{-3} mm^2/s from diffusion-weighted images allows for quantitative assessment of restricted diffusion. On ADC maps, low values—depicted as dark areas—represent restricted diffusion (Fig. 29.3). ADC maps are widely investigated in oncologic imaging to estimate response to neoadjuvant treatment [49, 50].

In an initial small study population of seven patients, pre-treatment ADC values were correlated to pathologic response grades [51]. However, in subsequent studies, the lack of technical standardization and methodologic variability proved challenging for quantifying robust thresholds of response. Two publications might demonstrate the heterogeneity of results with different techniques: in 2017, a single centre observation of 24 patients was performed on a 1.5 T unit with a b-value of 800 s/mm^2 [52]; in 2020 the same study group published a prospective assessment of 28 patients, using a 3 T MRI and a maximum b-value of 1000 s/mm^2 [53]. In the first study, a **pre-treatment** ADC value of $\geq 1.20 \times 10^{-3}$ mm^2/s was the strongest

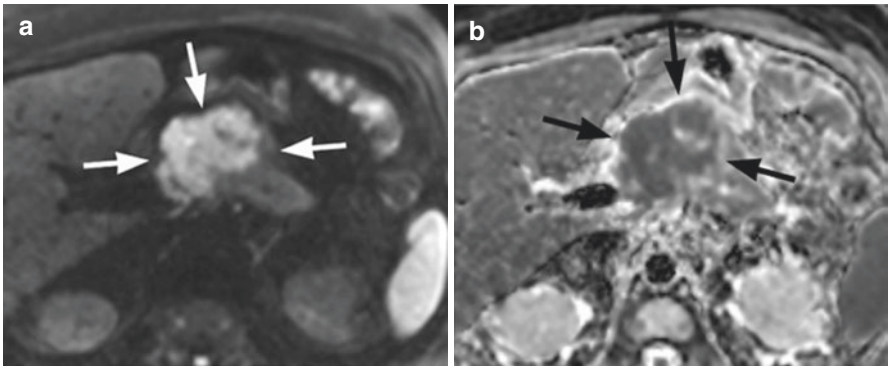

Fig. 29.3 Diffusion-weighted MR imaging. (**a**) Diffusion weighted image (DWI) of a PDAC at a b-value of 800 s/mm^2 reveals high signal intensities (arrows) as marker of restricted water diffusion within the tumour. The b-value describes intensity and time profile of the gradient pulse used. (**b**) Corresponding ADC map with predominantly low signal intensities (low ADC values) in the tumour area (arrows). Heterogeneity can also be noted

predictor for R0 resection (accuracy: 71%) and for pathologic response (accuracy: 83%; pathologic response defined as ≥30% tumour destruction). With 3 T MRI and b = 1000, the same parameter dropped in accuracy, but now **post-treatment** cut-off values of $\geq 1.40 \times 10^{-3}$ mm²/s emerged as strongest predictors: 75% accuracy for predicting R0 resection and 89% for histologic response. Additionally, patients with a post-treatment ADC of $\geq 1.40 \times 10^{-3}$ mm²/s had longer overall survival.

Another analysis of 23 patients with neoadjuvant therapy found an only moderate, although significant correlation of r = 0.517 (p = 0.02) between post-treatment ADC values and pathologic response grades [54]. Similar to prior studies, mean post-treatment ADC values were significantly higher, thus brighter than baseline values, and showed also an increase in standard deviation as a marker for supposed increasing tumour heterogeneity under therapy.

29.6.2 Tumour Heterogeneity, Definition of the Region of Interest and Future Developments

Assuming the concept of tumour heterogeneity, the definition of investigated tumour areas in terms of placing the Region of Interest (ROI) might explain the varying performance of pre- and post-treatment ADC values and ADC changes across papers. The selected ROI was either not described, encompassed the entire tumour volume, or was placed on one slice, with large vessels excluded.

The issue was addressed by another investigation with evaluation of both a selective ROI (the lowest ADC value, derived from the most diffusion-restricted area) and a ROI drawn over the entire tumour area, including necrosis. Both approaches used the slice with the largest tumour diameter [55] and only the relative change of ADC values under therapy was statistically evaluated. Not surprisingly, selective ADC values were more correlated to survival than whole-tumour-area ADC.

ADC values in a murine model with treated PDAC were inversely correlated to tumour "cellularity" [56]. This needs to be integrated with histopathologic knowledge of complex interactions between cellular stroma [19], inflammation and carcinoma cells. The differentiation of inflammation and adeno-carcinoma based on ADC values is still under debate and could be overcome by the generalized introduction of Intravoxel Incoherent Motion Diffusion-Weighted MRI (IVIM), a technique allowing for quantification of the fraction of flowing water in the microvasculature (perfusion fraction *f*, **see** Box 29.2) [57, 58]. In a preliminary work-up, the perfusion fraction was not useful to discriminate low/intermediate vs. high grade non-treated tumours [59], but a handful of papers confirmed the usefulness of IVIM for differentiating between PDAC and focal auto-immune

pancreatitis, owed to lower perfusion component in PDAC [60, 61]. Future investigation is needed to validate IVIM-DWI parameters for monitoring treatment response in PDAC [62].

Despite overlapping ADC values reported, there remains a strong consensus for routine application, that higher values ("brighter" ADC areas) are indicative for favourable tumour biology.

Similar to PET, requiring an interval of at least 4–5 weeks between NAT and restaging in order to allow restitution of actinic inflammation, MRI was performed within 3–5 weeks after completing NAT. Of note, in one publication MRI-ADC parameters outperformed the respective PET-SUV_{max} values [52].

Both functional methods may allow for estimating the overall response of a mass and predict survival [63], but they lack the spatial resolution to predict surgical margins around vessels. Still, in the light of evidence that pathologic response grade might be a factor associated with survival, biomarker imaging may play a role in future decision algorithms.

Box 29.2 IVIM (Intravoxel Incoherent Motion) MRI

IVIM imaging is a mathematical method to quantify all molecular motions contributing to a signal in Diffusion-weighted imaging (DWI). Apart from the molecular diffusion of water in tissue (true diffusion), water flowing in the capillary bed is the most important contributor to the signal, under the assumption of randomly orientated capillaries within a voxel (Fig. 29.4a). The signal component from water in the microvasculature is referred to as "pseudo-diffusion".

Different mathematical models have been proposed to separate true diffusion from microvascular blood flow [57, 58]. Using these algorithms, the contributing percentage of blood flow to a DWI signal and the perfusion fraction can be calculated and correlated to histology. Potential is seen e.g. in the quantification of neo-angiogenesis and monitoring of anti-angiogenetic drugs. Applications to pancreatic pathologies aimed at differentiating the poorly vascularized PDAC from atypical neuroendocrine neoplasms on imaging, or from focal auto-immune pancreatitis. IVIM-DW-MRI are prone to artefacts through image noise, respiratory and cardiac motion and to artefacts from gas in adjacent gastrointestinal structures.

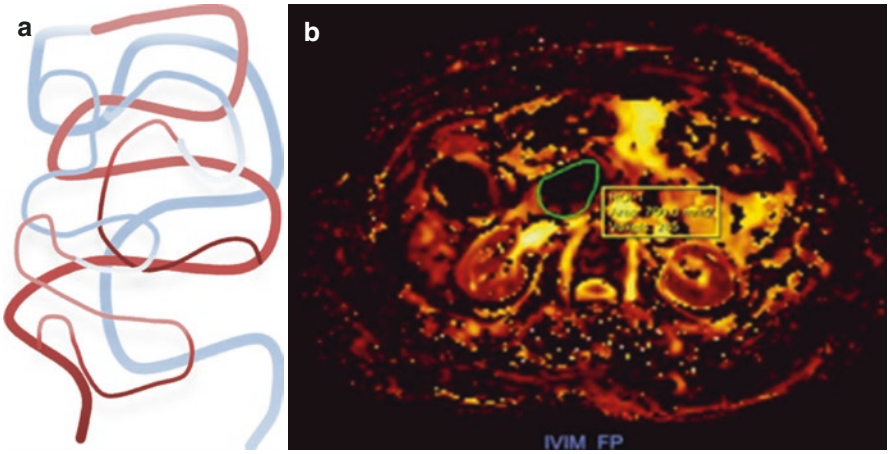

Fig. 29.4 Heterogeneous microvasculature in a tumour. (**a**) Randomly orientated capillaries within a voxel contribute to diffusion-weighted signals at lower b-values up to 600 s/mm^2 in the body. The effect becomes less important at high b-values. (**b**) IVIM perfusion fraction maps of a PDAC in the pancreatic head show a poorly vascularized lesion, encoded in dark colours. (From. De Robertis et al. [60])

29.7 Conclusion

The NCNN and ESMO panels currently endorse neoadjuvant therapy in borderline resectable PDAC [64, 65]. Several studies have shown that in a minority of patients, neoadjuvant therapy enabled R0 resection of locally advanced PDAC. However, histologic work-up suggests an inhomogeneous response of PDAC with interspersed carcinoma nests within stroma, extracellular matrix and inflammation. This poses a considerable challenge for interdisciplinary teams, to identify treated patients with potentially resectable disease.

According to current knowledge, RECIST1.1 partial response with radiologic mass regression occurs in a minority, while most patients remain stable on diagnostic imaging after neoadjuvant therapy. Generally, cross-sectional imaging overestimates the amount of residual viable tumour around vessels and thus cannot predict operability. There is no consistency across studies with regard to predictive imaging parameters for margin-free resection. Most studies are retrospective, single-centre, observational studies, examining changes in tumour size, vessel contact, or enhancement as hypotheses. Due to study heterogeneity, results are non-comparable, and statistical power is limited by small sample sizes. Though identification of potentially resectable patients is a rapidly evolving field in imaging research, at present, guidelines recommend taking patients to surgery after neoadjuvant therapy when there is no tumour progression on cross-sectional imaging [10, 66].

MR-DWI as a functional tool of MRI so far reveals conflicting results in the search for optimal threshold values of response. Also, while markers of low cellularity may be indicators of response, to date, functional imaging methods lack the spatial resolution to detect microscopic disease at the crucial interface of mass and vessel wall.

These limitations are thought to be overcome in the years ahead, and functional methods seems to harbour high potential for disease monitoring of treated pancreatic ductal adenocarcinoma.

References

1. Evans DB, George B, Tsai S. Non-metastatic pancreatic cancer: resectable, borderline resectable, and locally advanced-definitions of increasing importance for the optimal delivery of multimodality therapy. Ann Surg Oncol. 2015;22:3409–13.
2. Sugimoto M, Takahashi N, Farnell MB. Survival benefit of neoadjuvant therapy in patients with non-metastatic pancreatic ductal adenocarcinoma: a propensity matching and intention-to-treat analysis. J Surg Oncol. 2019;120:976.
3. Unno M, Hata T, Motoi F. Long-term outcome following neoadjuvant therapy for resectable and borderline resectable pancreatic cancer compared to upfront surgery: a meta-analysis of comparative studies by intention-to-treat analysis. Surg Today. 2019;49(4):295–9.
4. Katz MH, Pisters PW, Evans DB, Sun CC, Lee JE, Fleming JB, et al. Borderline resectable pancreatic cancer: the importance of this emerging stage of disease. J Am Coll Surg. 2008;206:833–46.
5. Sadot E, Doussot A, O'Reilly EM, Lowery MA, Goodman KA, Do RK, et al. FOLFIRINOX induction therapy for stage 3 pancreatic adenocarcinoma. Ann Surg Oncol. 2015;22(11):3512–21.
6. Mokdad AA, Minter RM, Zhu H. Neoadjuvant therapy followed by resection versus upfront resection for resectable pancreatic cancer: a propensity score matched analysis. J Clin Oncol. 2017;35(5):515–22.
7. Van Tienhoven GV, Versteijne E, Suker M, Groothuis KBC, Busch OR, Bonsing BA, et al. Preoperative chemoradiotherapy versus immediate surgery for resectable and borderline resectable pancreatic cancer (PREOPANC-1): a randomized, controlled, multicenter phase III trial. J Clin Oncol. 2018;36:LBA4002. https://doi.org/10.1200/JCO.2018.36.18_suppl.LBA4002.
8. Miyasaka Y, Ohtsuka T, Kimura R, Matsuda R, Mori Y, Nakata K, et al. Neoadjuvant chemotherapy with gemcitabine plus nab-paclitaxel for borderline resectable pancreatic cancer potentially improves survival and facilitates surgery. Ann Surg Oncol. 2019;26:1528–34.
9. Conroy T, Desseigne F, Ychou M, Bouché O, Guimbaud R, Bécouarn Y, et al. Groupe Tumeurs Digestives of Unicancer, PRODIGE intergroup. FOLFIRINOX versus gemcitabine for metastatic pancreatic cancer. N Engl J Med. 2011;364(19):1817–25.
10. Janssen QP, Buettner S, Suker M, Beumer BR, Addeo P, Bachellier P, et al. Neoadjuvant FOLFIRINOX in patients with borderline resectable pancreatic cancer: a systematic review and patient-level meta-analysis. J Natl Cancer Inst. 2019;111:782.
11. Schorn S, Demir IE, Reyes CM, Saricaoglu C, Samm N, Schirren R, et al. The impact of neoadjuvant therapy on the histopathological features of pancreatic ductal adenocarcinoma - a systematic review and meta-analysis. Cancer Treat Rev. 2017;55:96–106.
12. Scheufele F, Hartmann D, Friess H. Treatment of pancreatic cancer - neoadjuvant treatment in borderline resectable/locally advanced pancreatic cancer. Transl Gastroenterol Hepatol. 2019;4:32.

13. Katz MH. Response of borderline resectable pancreatic cancer to neoadjuvant therapy is not reflected by radiographic indicators. Cancer. 2012;118(23):5749–56.
14. Isaji S, et al. International consensus on definition and criteria of borderline resectable pancreatic ductal adenocarcinoma 2017. Pancreatology. 2018;18(1):2–11.
15. Siddiqui N, Vendrami CL, Chatterjee A, Miller FH. Advanced MR imaging techniques for pancreas imaging. Magn Reson Imaging Clin N Am. 2018;26(3):323–44.
16. Sasson AR, Wetherington RW, Hoffman JP, Ross EA, Cooper H, Meropol NJ, et al. Neoadjuvant chemoradiotherapy for adenocarcinoma of the pancreas: analysis of histopathology and outcome. Int J Gastrointest Cancer. 2003;34(2-3):121–8.
17. Evans DB, Rich TA, Byrd DR, Cleary KR, Connelly JH, Levin B, et al. Preoperative chemoradiation and pancreaticoduodenectomy for adenocarcinoma of the pancreas. Arch Surg. 1992;127:1335–9.
18. Hartman DJ, Krasinskas AM. Assessing treatment effect in pancreatic cancer. Arch Pathol Lab Med. 2012;136(1):100–9.
19. Kalimuthu SN, Serra S, Dhani N, Chetty R, et al. The spectrum of histopathological changes encountered in pancreatectomy specimens after neoadjuvant chemoradiation, including subtle and less-well-recognised changes. J Clin Pathol. 2016;69:463–71.
20. Lafaro KJ, Melstrom LG. The paradoxical web of pancreatic cancer tumor microenvironment. Am J Pathol. 2019;189(1):44–57.
21. Sherman WH, Hecht E, Leung D, Chu K. Predictors of response and survival in locally advanced adenocarcinoma of the pancreas following neoadjuvant GTX with or without radiation therapy. Oncologist. 2018;23(1):4–e10.
22. Chatterjee D, Katz MH, Rashid A, Wang H, Iuga AC, Varadhachary GR, et al. Perineural and intraneural invasion in posttherapy pancreaticoduodenectomy specimens predicts poor prognosis in patients with pancreatic ductal adenocarcinoma. Am J Surg Pathol. 2012;36(3):409–17.
23. Chatterjee D, Rashid A, Wang H, Katz MH, Wolff RA, Varadhachary GR, et al. Tumor invasion of muscular vessels predicts poor prognosis in patients with pancreatic ductal adenocarcinoma who have received neoadjuvant therapy and pancreaticoduodenectomy. Am J Surg Pathol. 2012;36(4):552–9.
24. Naito Y, Ishikawa H, Sadashima E, Okabe Y, Takahashi K, Kawahara R, et al. Significance of neoadjuvant chemoradiotherapy for borderline resectable pancreatic head cancer: pathological local invasion and microvessel invasion analysis. Mol Clin Oncol. 2019;11(3):225–33.
25. Versteijne E, Vogel JA, Besselink MG, Busch ORC, Wilmink JW, Daams JG, et al. Meta-analysis comparing upfront surgery with neoadjuvant treatment in patients with resectable or borderline resectable pancreatic cancer. Br J Surg. 2018;105(8):946–58.
26. Tang K, Lu W, Qin W, Wu Y. Neoadjuvant therapy for patients with borderline resectable pancreatic cancer: a systematic review and meta-analysis of response and resection percentages. Pancreatology. 2016;16(1):28–37.
27. Rombouts SJ, Walma MS, Vogel JA, van Rijssen LB, Wilmink JW, Mohammad NH, et al. Systematic review of resection rates and clinical outcomes after FOLFIRINOX-based treatment in patients with locally advanced pancreatic cancer. Ann Surg Oncol. 2016;23(13):4352–60.
28. Baliyan V, Kordbacheh H, Parakh A, Kambadakone A, et al. Response assessment in pancreatic ductal adenocarcinoma: role of imaging. Abdom Radiol. 2018;43:435–44.
29. Dhir M, Malhotra GK, Sohal DPS, Hein NA, Smith LM, O'Reilly EM, et al. Neoadjuvant treatment of pancreatic adenocarcinoma: a systematic review and meta-analysis of 5520 patients. World J Surg Oncol. 2017;15(1):18.
30. Xia BT, Fu B, Wang J, Kim Y, Ahmad SA, Dhar VK, et al. Does radiologic response correlate to pathologic response in patients undergoing neoadjuvant therapy for borderline resectable pancreatic malignancy? J Surg Oncol. 2017;115(4):376–83.
31. Amer AM, Zaid M, Chaudhury B, Elganainy D, Lee Y, Wilke CT, et al. Imaging-based biomarkers: changes in the tumour interface of pancreatic ductal adenocarcinoma on computed tomography scans indicate response to cytotoxic therapy. Cancer. 2018;124(8):1701–9.

32. Del Chiaro M, Søreide K. Trials and tribulations of neoadjuvant therapy in pancreatic cancer. Br J Surg. 2018;105(11):1387–9.
33. Petrelli F, Coinu A, Borgonovo K, Cabiddu M, Ghilardi M, Lonati V, et al. FOLFIRINOX-based neoadjuvant therapy in borderline resectable or unresectable pancreatic cancer: a meta-analytical review of published studies. Pancreas. 2015;44(4):515–21.
34. Suker M, Beumer BR, Sadot E, Marthey L, Faris JE, Mellon EA, et al. FOLFIRINOX for locally advanced pancreatic cancer: a systematic review and patient-level meta-analysis. Lancet Oncol. 2016;17(6):801–10.
35. Cassinotto C, Cortade J, Belleannée G, Lapuyade B, Terrebonne E, Vendrely V, et al. An evaluation of the accuracy of CT when determining resectability of pancreatic head adenocarcinoma after neoadjuvant treatment. Eur J Radiol. 2013;82(4):589–93.
36. Ferrone C, Marchegiani G, Hong TS, Ryan DP, Deshpande V, McDonnell EI, et al. Radiological and surgical implications of neoadjuvant treatment with FOLFIRINOX for locally advanced and borderline resectable pancreatic cancer. Ann Surg. 2015;261:12–7.
37. Wagner M, Antunes C, Pietrasz D, Cassinotto C, Zappa M, Sa Cunha A, et al. CT evaluation after neoadjuvant FOLFIRINOX chemotherapy for borderline and locally advanced pancreatic adenocarcinoma. Eur Radiol. 2017;27:3104–16.
38. Beleù A, Calabrese A, Rizzo G, Capelli P, Bellini N, Caloggero S. Preoperative imaging evaluation after downstaging of pancreatic ductal adenocarcinoma: a multi-center study. Cancers (Basel). 2019;11(2):E267. https://doi.org/10.3390/cancers11020267.
39. Cassinotto C, Mouries A, Lafourcade JP, Terrebonne E, Belleannée G, Blanc JF, et al. Locally advanced pancreatic adenocarcinoma: reassessment of response with CT after neoadjuvant CRT. Radiology. 2014;273(1):108–16.
40. Michelakos T, Pergolini I, Castillo CF, Honselmann KC, Cai L, Deshpande V. Predictors of resectability and survival in patients with borderline and locally advanced pancreatic cancer who underwent neoadjuvant treatment with FOLFIRINOX. Ann Surg. 2019;269(4):733–40.
41. Somers I, Bipat S. Contrast-enhanced CT in determining resectability in patients with pancreatic carcinoma: a meta-analysis of the positive predictive values of CT. Eur Radiol. 2017;27:3408–35.
42. Ganeshan B, Miles KA. Quantifying tumour heterogeneity with CT. Cancer Imaging. 2013;13:140–9.
43. Lubner MG, Stabo N, Lubner SJ, del Rio AM, Song C, Halberg RB, et al. CT textural analysis of hepatic metastatic colorectal cancer: pre-treatment tumour heterogeneity correlates with pathology and clinical outcomes. Abdom Imaging. 2015;40(7):2331–7.
44. Lubner MG, Smith AD, Sandrasegaran K, Sahani DV, Pickhardt PJ, et al. CT texture analysis: definitions, applications, biologic correlates, and challenges. Radiographics. 2017;37(5):1483–503.
45. Cheng SH, Cheng YJ, Jin ZY, Xue HD, et al. Unresectable pancreatic ductal adenocarcinoma: role of CT quantitative imaging biomarkers for predicting outcomes of patients treated with chemotherapy. Eur J Radiol. 2019;113:188–97.
46. Summers RM. Texture analysis in radiology: does the emperor have no clothes? Abdom Radiol. 2017;42(2):342–5.
47. Yamashita R, Perrin T, Chakraborty J, Chou JF, Horvat N, Koszalka MA, et al. Radiomic feature reproducibility in contrast-enhanced CT of the pancreas is affected by variabilities in scan parameters and manual segmentation. Eur Radiol. 2019;30:195.
48. Thoeny HC, Ross BD. Predicting and monitoring cancer treatment response with DW-MRI. J Magn Reson Imaging. 2010;32(1):2–16.
49. Amodeo S, Rosman AS, Desiato V, et al. MRI-based apparent diffusion coefficient for predicting pathologic response of rectal cancer after neoadjuvant therapy: systematic review and meta-analysis. AJR Am J Roentgenol. 2018;211(5):W205–W16.
50. ACRIN 6698 Trial Team and I-SPY 2 Trial Investigators, Partridge SC, Zhang Z, Newitt DC, et al. Diffusion-weighted MRI findings predict pathologic response in neoadjuvant treatment of breast cancer: the ACRIN 6698 multicenter trial. Radiology. 2018;289(3):618–27.

51. Cuneo KC, Chenevert TL, Ben-Josef E, Feng MU, Greenson JK, Hussain HK, et al. A pilot study of diffusion-weighted MRI in patients undergoing neoadjuvant chemoradiation for pancreatic cancer. Transl Oncol. 2014;7:644–9.
52. Okada KI, Hirono S, Kawai M, Miyazawa M, Shimizu A, Kitahata Y, et al. Value of apparent diffusion coefficient prior to neoadjuvant therapy is a predictor of histologic response in patients with borderline resectable pancreatic carcinoma. J Hepatobil Pancreat Sci. 2017;24(3):161–8.
53. Okada KI, Kawai M, Hirono S, Kojima F, Tanioka K, Terada M, et al. Diffusion-weighted MRI predicts the histologic response for neoadjuvant therapy in patients with pancreatic cancer: a prospective study (DIFFERENT trial). Langenbeck's Arch Surg. 2020;405(1):23–33.
54. Dalah E, Erickson B, Oshima K, Feng MU, Greenson JK, Hussain HK, et al. Correlation of ADC with pathological treatment response for radiation therapy of pancreatic cancer. Transl Oncol. 2018;11(2):391–8.
55. Nishiofuku H, Tanaka T, Marugami N, Sho M, Akahori T, Nakajima Y, et al. Increased tumour ADC value during chemotherapy predicts improved survival in unresectable pancreatic cancer. Eur Radiol. 2016;26:1835–42.
56. Heid I, Steiger K, Trajkovic-Arsic M, Settles M, Eßwein MR, Erkan M, et al. Co-clinical assessment of tumor cellularity in pancreatic cancer. Clin Cancer Res. 2017;23(6):1461–70.
57. Iima M, Le Bihan D. Clinical intravoxel incoherent motion and diffusion MR imaging: past, present, and future. Radiology. 2016;278(1):13–32.
58. Le Bihan D. What can we see with IVIM MRI? NeuroImage. 2019;187:56–67.
59. Ma C, Li Y, Wang L, Wang Y, Zhang Y, Wang H, et al. Intravoxel incoherent motion DWI of the pancreatic adenocarcinomas: monoexponential and biexponential apparent diffusion parameters and histopathological correlations. Cancer Imaging. 2017;17(1):12.
60. De Robertis R, Cardobi N, Ortolani S, Tinazzi Martini P, Stemmer A, et al. Intravoxel incoherent motion diffusion-weighted MR imaging of solid pancreatic masses: reliability and usefulness for characterization. Abdom Radiol. 2019;44(1):131–9.
61. Klauss M, Lemke A, Grünberg K, Simon D, Re TJ, Wente MN, et al. Intravoxel incoherent motion MRI for the differentiation between mass forming chronic pancreatitis and pancreatic carcinoma. Investig Radiol. 2011;46(1):57–63.
62. Klaassen R, Gurney-Champion OJ, Engelbrecht MRW, Stoker J, Wilmink JW, Besselink MG, et al. Evaluation of six diffusion-weighted MRI models for assessing effects of neoadjuvant chemoradiation in pancreatic cancer patients. Int J Radiat Oncol Biol Phys. 2018;102(4):1052–62.
63. Kurosawa J, Tawada K, Mikata R, Ishihara T, Tsuyuguchi T, Saito M, et al. Prognostic relevance of apparent diffusion coefficient obtained by diffusion-weighted MRI in pancreatic cancer. J Magn Reson Imaging. 2015;42(6):1532–7.
64. National Comprehensive Cancer Network. NCCN clinical practice guidelines in oncology. Pancreatic adenocarcinoma. Version 2.2017. J Natl Compr Cancer Netw. 2017;15(8):1028–61.
65. Ducreux M, Cuhna AS, Caramella C, Hollebecque A, Burtin P, Goéré D, Seufferlein T, Haustermans K, Van Laethem JL, Conroy T, Arnold D. Cancer of the pancreas: ESMO Clinical Practice Guidelines for diagnosis, treatment and follow-up. Ann Oncol. 2015;26(Suppl 5):v56–68.
66. Isaji S, Mizuno S, Windsor JA, Bassi C, Fernández-Del Castillo C, Hackert T, Hayasaki A, Katz MHG, Kim SW, Kishiwada M, et al. International consensus on definition and criteria of borderline resectable pancreatic ductal adenocarcinoma 2017. Pancreatology. 2018;18(1):2–11.